

EGTSyn: Edge-based Graph Transformer for Anti-Cancer Drug Combination Synergy Prediction

Jie Hu¹, Xiaozhi Zhang², Desi Shang³, Lijun Ouyang¹, Yue Li¹, Dongping Xiong^{1*}

¹School of Computer science/Software, University of South China, Hunan 421001, China;

²School of Electrical Engineering, University of South China, Hunan 421001, China;

³The First Affiliated Hospital, Hengyang Medical School, University of South China, Hunan 421001, China.

Keywords: Anti-cancer drug combination, Drug synergy prediction, Cancer therapy, Deep learning, Edge-based Graph Neural Network, Transformer;

Abstract

Combination therapy with multiple drugs is a potent therapy strategy for complex diseases such as cancer, due to its therapeutic efficacy and potential for reducing side effects. However, the extensive search space of drug combinations makes it challenging to screen all combinations experimentally. To address this issue, computational methods have been developed to identify prioritized drug combinations. Recently, Convolutional Neural Networks based deep learning methods have shown great potential in this community. Although the significant progress has been achieved by existing computational models, they have overlooked the important high-level semantic information and significant chemical bond features of drugs. It is worth noting that such information is rich and it can be represented by the edges of graphs in drug combination predictions. In this work, we propose a novel Edge-based Graph Transformer, named EGTSyn, for effective anti-cancer drug combination synergy prediction. In EGTSyn, a special Edge-based Graph Neural Network (EGNN) is designed to capture the global structural information of chemicals and the important information of chemical bonds, which have been neglected by most previous studies. Furthermore, we design a Graph Transformer for drugs (GTD) that combines the EGNN module with a Transformer-architecture encoder to extract high-level semantic information of drugs. The proposed EGTSyn is highly capable of capturing the global chemical information and corresponding carcinoma cell line gene profiles for more accurate synergistic judgement of drug combinations. We compare the EGTSyn with classical machine learning based-models and state-of-the-art deep learning-based models, and the experiment results demonstrate that the EGTSyn outperforms these competitive methods. Leave-one-out experiments are also conducted and the results are all quite positive. Moreover, we test our trained model on unseen drug pairs, which verifies the superior generalization performance of EGTSyn.

1 Introduction

Cancer is one of the leading causes of death. According to the Global Cancer Observatory statistics for 2020 by the International Agency for Research on Cancer (IARC), approximately 19.3 million new cancer patients were reported, and 10 million deaths were recorded (Ferlay et al., 2021). Since a single drug therapy is inadequate to manage the evolution of therapy resistance, drug combination therapy has been developed to tackle these complex diseases (Chatterjee and Bivona, 2019). In recent years, synergistic drug combinations have been successfully and rapidly developed. Synergistic combinations of drugs perform better therapeutic efficacy than the addictive monotherapy (Roell et al., 2017). These

combinations have been successfully applied in the treatment of various tumors, such as the human HER2-positive breast cancer (Bazgir et al., 2018), chronic myeloid leukemia (Westerweel et al., 2019), castration-resistant prostate cancer (Xu and Qiu, 2019), and BRAF-mutated tumors (Ribas et al., 2019). Drug combination therapy has the advantage of reducing adverse side effects and host toxicity by using a smaller dosage per drug. Additionally, the therapy of multiple drug combinations can suppress or even overcome drug resistance (Huang et al., 2017). However, some drug combinations may have negative effects and even aggravate the disease (Azam and Vazquez, 2021). Therefore, discovering synergistic combinations of drugs is a significant task in anti-cancer therapy.

Traditionally, clinical experience and high-throughput screening (HTS) are two common methods for finding synergistic drug combinations. However, the clinical method is time-consuming and labor-intensive, and it may unnecessarily put the health of patients at risk. To prioritize drug combinations, some HTS methods that utilize the diversity of chemical features and omics data have also been proposed (Torres et al., 2013; Menden et al., 2019; Kragh et al., 2021). Nevertheless, experimentally testing all potential drug combinations using HTS is impractical, since the synergy between drugs is rare (Jaaks et al., 2022). With the number of anti-cancer drugs dramatically increasing, the drug combination space has become enormous.

Recently, many large-scale datasets for drug combinations have been released, such as drug datasets DrugCombDB (Zagidullin et al., 2019) and DrugBank (Wishart et al., 2018), gene expression dataset Cancer Cell Line Encyclopedia (CCLE) (Barretina et al., 2012) and screening synergy drug pairs datasets O’Neil (O’Neil et al., 2016). These datasets have led to the development of various computational methods for efficiently screening synergistic drug combinations at low cost. Initially, traditional machine learning based methods were developed to predict synergistic drug combinations, such as Random Forests (Gayvert et al., 2017; Nakano and JB, 2020), gradient boosting (Zagidullin et al., 2021), ensemble learning (Preto et al., 2022), and XGBoost (Meng et al., 2022).

More recently, deep learning has made incremental advancements in predicting synergistic drug combinations and has generally performed better than machine learning-based methods. Fully Connected Networks (FCNs) were initially applied to discover novel drug pairs. For instance, DeepSynergy (Preuer et al., 2018) utilized a deep neural network model with chemical fingerprints information and genomic profiles for the synergistic effect prediction tasks. Two other FCNs based methods (Kuru et al., 2021; Kim et al., 2021) were also proposed after that. Kuru *et al.* (Kuru et al., 2021) proposed a deep learning method using gene expression profiles of cancer cell lines and drug chemical descriptors information, while Kim Y *et al.* (Kim et al., 2021) attempted to utilize multitask deep neural networks to learn the interaction between cancer cell lines and drugs, and transfer learning to make the synergistic effect prediction in data-poor tissues. In addition, Convolutional Neural Networks (CNNs) and Transformers have also employed for drug discovery tasks. REFINED (Bazgir et al., 2021) and TranSynergy (Liu and Xie, 2021) are the representative methods for synergistic drug combination prediction. The former took drug descriptors into account and transformed them into image-forms, and then utilized the CNN framework to model drug combination effects. While the latter employed a Transformer and FCN layers to explicitly model the cellular effect of drug actions. More recently, Graph Neural Network (GNN) has attracted more attention in drug discovery community. For example, GraphDTA (Nguyen et al., 2021) represented the drugs as graphs and utilized GNN to extract drug features. In the follow-up studies, DeepDDs (Wang et al., 2022) and DTSyn (Hu et al., 2022) learned the drug graph representation from the chemical SMILE structures where the atom is node and chemical bond is edge. GraphSynergy (Yang et al., 2021) and Jiang *et al.* (Jiang et al., 2020) encoded the information of multimodal data in a graph to learn the interaction of drugs. Additionally,

HypergraphSynergy (Liu et al., 2022) formulated the identification of synergistic drug combinations over cancer cell lines as a hypergraph representation learning to promote novel cancer drug discoveries.

Although GNN-based methods have demonstrated superior performance in drug discovery and prediction, they often overlook the importance of chemical bond features that contain valuable information in drug combination predictions. The two recent proposed GNN models, NENN (Yang and Li, 2020) and EGATs (Wang et al., 2021), have incorporated the edge information into graph feature representations, and have proven highly competitive against other approaches in the same tasks. Mastropietro A *et al.* have also interpreted the importance of edge information in graphs from a medical perspective (Mastropietro et al., 2022). Moreover, recent studies integrating GNN with Transformer for molecule structure modelling have achieved great success in molecular prediction tasks (Rong et al., 2020; Atz et al., 2021; Kearnes et al., 2016), and indicated the superiority of GNN-based Transformer architecture.

Inspired by the above studies, this work proposes a novel Edge-based Graph Transformer, named EGTSyn, for effective anti-cancer drug combination synergy prediction. First, we design an Edge-based Graph Neural Network (EGNN) module, which is employed to capture the global structure information of the chemicals as well as the important chemical bond features. They are always neglected in previous studies. Second, we combine the EGNN module with a Transformer architecture encoder to extract high-level semantic information of drugs, denoted as Graph Transformer for Drugs (GTD) block. Furthermore, we concatenate the high-level semantic information and low-level structural information using a long-distance residual connection in GTD block to convey initial atom-bond structure information. In this way, EGTSyn is highly capable of capturing the global chemical information and corresponding carcinoma cell line gene profiles for more accurate synergetic judgement of drug combinations.

We compare the EGTSyn with baseline methods, including state-of-the-art models DeepDDS, DeepSynergy, TranSynergy, and classical machine learning methods. Furthermore, we implement a random split 5-folds cross validation on the benchmark dataset, and the results demonstrate that EGTSyn outperforms these competitive baselines. We also conduct leave-drugs-out, leave-tissue-out, and leave-drugs combination-out testing to further verify the performance of the proposed model, and the results are positive. Additionally, we test our trained model on unseen drug pairs, and the results validate the superior generalization ability of EGTSyn. As demonstrated by these experiments, the proposed EGTSyn model exhibits excellent performance for predicting anti-cancer drug combination synergistic effects and holds great promise for further wet-lab research.

2 Materials and Methods

2.1 Data collections

The benchmark dataset of drug synergistic combinations are obtained from an oncology screening dataset that is released by recent studies (Wang et al., 2022; O’Neil et al., 2016). Conditioned by cancer cell line expression data, 12415 drug pairs are selected to build the benchmark dataset and it covers 31 human cancer cell lines and 36 anti-cancer drugs. The degree of synergy is evaluated using the Loewe Activity score, which is calculated based on the Loewe Additivity model (Loewe, 1953). A drug pair with a Loewe score greater than zero is considered synergistic, while those with a score less than zero are considered antagonistic. The higher the Loewe score of a drug pair, the more effective it is for clinical therapy. To account for noisy data and labels (Wang et al., 2022), a synergy threshold of 10 is chosen. The drug pairs that have a Loewe score greater than 10 are labeled as positive, while those has a Loewe score less than zero are labeled as negative.

The drug features are formulated using a process illustrated in **Figure 1(a)**. The chemical SMILES (Weininger, 1988) of drugs are obtained from the DrugBank database (Wishart et al., 2018). Then, the chemical structural formula of each drug is reformulated using RDKit (Landrum, 2013) and converted into graphs based on the chemical structural formula. In these graphs, atoms and chemical bonds are represented as nodes and edges, respectively. The feature vectors of atoms include information such as atom symbol, number of adjacent atoms, aromaticity, valence, and number of adjacent hydrogens. Chemical bond feature vectors are encoded based on the bond type, direction of the bond, conjugation, aromaticity, ring, and owning molecule.

In this study, the gene expression profiles of carcinoma cell lines are derived from Cancer Cell Line Encyclopedia (CCLE) (Barretina et al., 2012), which is employed to characterize mRNA expression data, genomes and anti-cancer drug dose responses across carcinoma cell lines. Representative genes are extracted from the original gene expressions based on the LINCS project (Yang et al., 2012). This project provides approximately 1000 well-chosen genes that cover 80% of the gene information, building upon the Connectivity Map (CMap) data (Cheng and Li, 2016). The process of acquired gene expression data is depicted in **Figure 1(b)**.

2.2 Cancer cell line feature extraction

There are totally 954 numeric features have been selected from raw gene expression data as the inputs of cell line feature reduction block, as illustrated in **Figure 2**. This block consists of a two-layer MLP and a fully connected layer. The computation for generating cancer cell line feature embeddings can be formulated as

$$\begin{aligned} O_1 &= \text{Dropout}(\sigma(xW_1 + b_1)), \\ O_2 &= \text{Dropout}(\sigma(O_1W_2 + b_2)), \\ x' &= \sigma(O_2W_3 + b_3), \end{aligned} \tag{1}$$

where x denotes the input cancer cell line features, $\text{Dropout}(\cdot)$ denotes a dropout layer, $\sigma(\cdot)$ denotes an activation function, such as ReLU, W_1, W_2, W_3 represent the weights, b_1, b_2, b_3 are the biases and x' is the output embeddings, respectively. Following processing by the cell line feature reduction block, the feature embeddings of a specific cell line can be extracted.

2.3 Chemical feature representation

EGTSyn adopts a molecule-based representation for drugs, where a molecule is composed of atoms and chemical bonds. The graph representation of a molecule consists of nodes that correspond to atoms and edges that correspond to chemical bonds. Each atom is characterized by its symbol, the number of adjacent atoms, aromaticity, valence, and the number of adjacent hydrogens. Details regarding atom features are tabulated in **Table 1**. Similarly, the features of a chemical bond include bond type, direction, conjugation, aromaticity, ring, and owning molecule. Further information about bond features can be found in **Table 2**.

In this work, both atoms and chemical bonds of drugs are converted to nodes and served as the inputs of our model. The combination of these two kinds of nodes enables richer global features to be captured and is expected to be beneficial. More details will be demonstrated in the ablation study.

2.4 Workflow of our method

The architecture of EGTSyn is depicted in **Figure 3**. The inputs of the model include two chemical structural SMILES (Weininger, 1988) of drug pairs and an untreated cancer cell line expression gene profile. The drug feature graphs constructed from the SMILES input are processed by our GTD block which employs an EGNN and a Transformer-based encoder to generate drug embeddings. Then the cell line feature reduction block encodes the gene expression profile of cancer cell line. Finally, the obtained drug embeddings and cell line embeddings are concatenated to form two separated drug-cell feature representation vectors. These vectors are then concatenated into a single vector and forward propagated to a fully connected layers for further processing, ultimately resulting in the final prediction label.

2.5 GTD block

The GTD block is an encoder block based on the Transformer architecture. It takes the chemical feature information of drugs as input and employs an EGNN module to encode the inputs into intermediate output embeddings. The output intermediate embeddings are formulated using a multi-head attention block followed by a feedforward layer. The pipeline of GTD block is depicted in **Figure 4**. Further details of these blocks are discussed in the following subsections.

2.5.1 GNN and GCN

A graph with node set V and edge set E can be denoted as $G = (V, E)$, where $E \in V \times V$. Specifically, $N_v = |V|$ and $N_e = |E|$ denote the number of nodes and edges, respectively. The adjacency matrix $A \in \mathbb{R}^{N_v \times N_v}$ represents the connectivity between nodes, where each element $A(i, j)$ corresponds to the connectivity of node i and node j , with $i, j \in V = \{n_1, n_2, \dots, n_{N_v}\}$. The node feature matrix $X \in \mathbb{R}^{N_v \times d_v}$ associates each node with a d_v dimensional feature vector. For a GNN, each node updates its representation by aggregating representations of its neighbors layer by layer. The input of a GNN is a node feature matrix X along with an adjacency matrix A and the output is a new node feature matrix $X' \in \mathbb{R}^{N_v \times d}$. The nodes of each layer are computed by the same function as

$$X' = f(X, \psi), \quad (2)$$

where d denotes the output feature dimension, f is an activation function, and ψ is an aggregate function.

The design of f and ψ distinguishes the types of GNNs to a large extent. A Graph Convolutional Network (GCN) (Kipf and Welling, 2016) is a kind of GNN and a multi-layer GCN can be propagated according to the following rule

$$H^{(l+1)} = \sigma(\tilde{D}^{-\frac{1}{2}} \tilde{A} \tilde{D}^{-\frac{1}{2}} H^{(l)} W^{(l)}), \quad (3)$$

where $H^{(l)}$ denotes the input matrix of l -th layer and $H^{(l+1)}$ represents the outputs of $(l + 1)$ -th layer. $\tilde{A} = \tilde{A} + I_N$ (I_N is identity matrix) is the adjacency matrix with self-connections, and $\tilde{D}_{ii} = \sum_j \tilde{A}_{ij}$. Additionally, W^l is a learnable weight matrix of a specific layer, and $\sigma(\cdot)$ denotes an activation function, such as ReLU.

2.5.2 EGNN

The EGNN module utilizes GCN layers with ReLU activation function to extract the graph features. As illustrated in **Figure 5**, two types of graphs are constructed, namely the atom-based graph and the atom-bond-based graph, which serve as inputs for EGNN. The atom-based graph that expresses the

structure information of chemicals uses nodes to represent atoms and edges to indicate chemical bonds. The designed atom-bond-based graph treats both the atoms and bonds as nodes, with the relations between them being regarded as edges. In this way, EGNN is capable of capturing both the structure information of chemicals and the global feature information including the importance of chemical bonds, which has been previously neglected by most studies. For example, an atom-bond-based edge is created between a specific atom and a particular chemical bond in the atom-bond-based graph, if the atom is linked to other atoms via the chemical bond.

Both graphs are processed as inputs by EGNN, and computed parallelly by the GCN block, respectively. The corresponding outputs are concatenated as the intermediate output embeddings for the subsequent Transformer encoder block. The original GCN is designed for node-level tasks while the drug combinations synergy prediction is a graph-level task. We thereby utilize sum, average and max pooling operations to obtain the whole graph feature information from the trained node and edge features. Then the aggregated graph features are used to estimate the performances. We observe that the max pooling operation in the proposed EGTSyn is superior to other operations. Hence, a global max pooling layer is added after the GCN layer to extract graph representations.

2.5.3 Transformer encoder

The Transformer encoder is built mainly upon the original implementation of Transformer (Vaswani et al., 2017), of which the self-attention layer is the basic module. The Transformer encoder stacks multiple scale-dot attention layer to formulate multi-head attention. In the GTD block, a group of queries, keys, values (q, k, v) are taken as the inputs of the self-attention layer. And the q, k and v are the extracted intermediate embeddings of EGNN. The outputs of scale-dot attention can be formulated as

$$\text{Attention}(Q, K, V) = \text{softmax}(QK^T / \sqrt{d})V, \quad (4)$$

where d is the dimension of q and k . Assume there are j attention layers in a multi-head self-attention module, then the output matrix is

$$\begin{aligned} \text{MultiHead}(Q, K, V) &= \text{Concat}(\text{head}_1, \dots, \text{head}_j)W^o, \\ \text{head}_i &= \text{Attention}(QW_i^Q, KW_i^K, VW_i^V), \end{aligned} \quad (5)$$

where W_i^Q, W_i^K, W_i^V are the projection matrices of head i .

It should be noticed that the inputs of a typical self-attention block should be vectorized, such as that in Equation (4). However, in fact, the input data of graph is generally not vectorized. Inspired by the previous studies (Vaswani et al., 2017; Atz et al., 2021; Ying et al., 2021), we take the extracted vectors pipelined by EGNN as keys, queries and values of the Transformer encoder. The keys, queries, values are then processed by Scaled Dot-Product Attention (Vaswani et al., 2017) with a layer normalization (LN) (Xiong et al., 2020). Additionally, we apply a long-distance residual connection structure which concatenates the embeddings processed by EGNN module to convey the initial atom-bond structure information. Finally, the processed vectors are fed into a feed-forward layer (FFN). In a sense, the residual structure fuses the original structure information between atom-atom and atom-bond, and the second-level semantic information.

The GTD block comprises the EGNN module and a Transformer encoder block, as depicted in **Figure 4**.

2.6 Predictions

After being preconditioned, the drug representations are fed into the GTD block and the cancer cell line representations are fed into feature reduction block. After pipelined by their respective modules, the cell line gene expression features are concatenated to drug A and drug B embeddings, yielding representations for cell line-drug A and cell line-drug B. These two representations are then concatenated together to generate the final representation, which is subsequently fed into the classify layer to predict whether synergy is present or not.

In EGTSyn, we adopt the cross-entropy as the loss function, which can be formulated as

$$\text{Loss} = \min \left(-\sum_{n=1}^N \log P_n + \frac{2}{\delta} \|\theta\| \right). \quad (6)$$

Where θ refers to all learnable parameters of weight and bias, N is the number of all training samples, δ is L_2 norm parameter, while P_n is the predicted possibility of the n -th label.

3 Results

3.1 Hyperparameter settings

In EGTSyn, the dimension of chemical atom and eigenvectors of chemical bonds are both set to 78, while the dimension of cell line is set to 945. The hyperparameters of our EGTSyn are presented in **Table 3**. Given the vast search space of the hyperparameters, we employ grid-search as a means to tune the parameters of our model, conducting experiments via five-fold cross-validation on our benchmark dataset. As demonstrated in **Table 3**, we conduct a series of experiments with different EGCN layer, EGCN size, GTDblock hidden size, number of attention heads, as well as the size of cell line feature reduction block MLP and final linear prediction block. For dropout rate and learning rate, there are multiple values to be evaluated on them. Considering global drug feature, we apply three graph pool methods to our model and find that the max feature aggregation method behaved better. The best values of these parameters tested on our benchmark dataset are demonstrated in boldface.

3.2 Performance metrics

We frame drug combination synergy prediction as classification tasks, with a label of 1 denoting synergistic drug combinations and a label of 0 indicating the opposite. The measurement metrics include ROC-AUC (the receiver operator characteristics curve), PR-AUC (the area under the precision-recall curve), ACC (accuracy), BACC (balanced accuracy), PREC (precision), TPR (True Positive Rate) and the KAPPA (Cohen’s Kappa value).

3.3 Comparison methods

We adopt several baseline models for comparison with our proposed EGTSyn. The baseline models include the top-ranking deep learning-based models and classical machine learning-based models. Specifically, we consider four deep methods, namely MLP, DeepSynergy, TranSynergy, as well as DeepDDS, and three classical machine learning-based methods, namely Support Vector Machine (SVM), Random Forest (RF), and Adaboost. To evaluate the performance of the proposed approach, we compare it with the baseline methods that are configured with the best parameters on our benchmark dataset. We employ 5-fold cross-validation and evaluate the leave-drugs-out, leave-tissue-out, and leave-drug combination-out experiments, respectively.

3.4 Experiment results

The proposed EGTSyn is firstly compared to the baseline models upon the random split 5-folds cross validation. The comparison results are shown in **Table 4**, where EGTSyn achieves ACC, BACC, PREC, ROC AUC, PR AUC, TPR, and Kappa values of 0.87, 0.87, 0.89, 0.94, 0.93, 0.90, and 0.73, respectively. The results indicate that our model vastly outperforms the traditional machine learning based models and is superior to the state-of-art deep learning-based model DeepDDS. It is worth noting that the performance evaluation of EGTSyn is superior to the compared baseline methods across all performance metrics as depicted in **Figure 6**. Besides, we conduct an experiment to measure the performance of our EGTSyn with different input orders of two drugs and find that our EGTSyn achieves ACC, BACC, PREC, ROC AUC, PR AUC, TPR, and Kappa of 0.85, 0.85, 0.88, 0.92, 0.92, 0.86, 0.70 respectively. These results suggest that our proposed model is robust and not affected by the drug sequence.

As the previous studies, we conduct leave-drugs-out, leave-tissue-out and leave-drug combinations-out experiments to further verify the performance of EGTSyn. The experiment results are demonstrated in **Table 5**, where the EGTSyn outperforms competitive baseline models. For leave-drugs-out, we utilize 5-fold cross validation to evaluate the model. Specifically, we divide the dataset into five subsets of approximately equal size based on different drugs, and each subset is used as test a dataset in turn while the remaining four subsets are employed as training sets. The average score of the 5-fold is utilized as the final predictions. As shown in **Table 5**, EGTSyn performs better than these competitive baseline methods. For leave-tissue-out, we iteratively remove all the cancer cell lines belonging to specific tissue from our benchmark dataset and use these cell lines as test set while the remaining samples are used as train dataset. **Table 5** illustrates that EGTSyn achieves the best performance when the gene information is not available in test set. Furthermore, **Figure 7** demonstrates the superior performance of EGTSyn compared to three other deep learning methods (MLP, DeepDDS, and DeepSynergy) in terms of the ACC metric on six different cancer tissues. Specifically, EGTSyn achieves ACC values of 0.76, 0.802, 0.758, 0.771, 0.759, and 0.726, respectively, which are better than those achieved by the other methods. For leave-drugs combination-out, we iteratively choose some different drug combinations from the bench mark dataset and use the remaining samples to train the model. Then the trained model is evaluated on the chosen combinations. As shown in **Table 5**, the results of EGTSyn differ only slightly from that of DeepDDS but get less variance, which indicates the stability of the proposed model.

3.5 Ablation study

In this part, we conduct ablation experiments to quantify the contribution of individual design components of EGTSyn on our benchmark dataset. The results of ablation experiments are illustrated in **Table 6**. Three variants derived from EGTSyn model are introduced as follows:

No edge encoding. We remove the edge encoding block from our model and name the resulting model GTSyn. This model utilizes only node embeddings, which are passed through a graph-based message passing network and then a Transformer encoder.

No Transformer encoding. In this variant, we remove the multi-head self-attention mechanism from our model and name it EGSyn. The EGSyn model encodes only the atom feature and the atom-bond feature, which are then separately passed to the graph-based message passing network. The outputs of the network are concatenated and passed through a pipeline block comprising several fully connected layers.

No both edge and Transformer encoding. To demonstrate the effectiveness of the combination of the two proposed modules, we remove both the Transformer encoder and the edge encoder from the EGTSyn model. We name it as GSyn, which employs only node embeddings and a graph-based message passing network for chemical feature extraction.

As shown in **Table 6**, the performance of our EGTSyn model is superior to that of the other three variants which indicates the fact that both the edge encoder module with information on chemical bonds and the self-attention mechanism module in our model contribute to final performance. Notably, GSyn has the lowest performance among the four models. GTSyn outperforms EGTSyn slightly in some metrics, which suggests that the Transformer encoder appears to have a more significant impact on the overall performance of our method compared to the edge encoder module.

3.6 Case study

The above results have proved the competency of our model. Next, to further discuss the prediction ability and generalization performance of the model, we train the proposed EGTSyn on our benchmark dataset and then conduct the following experiments.

Performance evaluation of predictive ability. We select the T-47D cell line (Yu et al., 2017), a human breast cancer cell line known for its hormonal expression of cancer cells, as a representative example to compare the predictive scores of our trained model with its actual synergy scores. Specifically, the T-47D dataset consists of 440 drug pairs, approximately half of which are synergistic (labeled as 1) and the remaining half are antagonistic (labeled as 0). The prediction results are demonstrated in **Figure 8(a)**, and our conclusions are as follows. Firstly, most of the drug pairs that have a synergy score bigger than 0 are predicted as synergistic, while the samples that have a synergy score less than 0 are predicted as non-synergistic. Secondly, the higher the true synergy score is, the larger the predict possibility is, and the more possible of the sample will be labeled as positive by our model. These observations confirm the effectiveness and high prediction accuracy of EGTSyn.

Evaluation on independent datasets. To validate the generalization performance of the proposed model, we first train the model EGTSyn on the benchmark data set, and then apply it in the prediction of three new independent datasets, including Wang’s (Wang et al., 2022), Menden’s (Menden et al., 2019) and Liu’s (Liu et al., 2022). The Wang’s dataset contains 162 drug pairs and covers 22 Carcinoma cell lines as well as 40 kinds of drugs. The Menden’s dataset contains 1008 drug pairs and covers 24 Carcinoma cell lines as well as 55 kinds of drugs, and the Liu’s dataset contains 18950 drug pairs and covers 39 Carcinoma cell lines as well as 38 unique drugs. In these datasets, the drug combination pairs that exist in the training data are removed. The generated three new independent datasets are tested by EGTSyn and the results are displayed in **Figure 8(b)**. We focus on the ACC score as it reflects the accuracy of the drug combination synergy prediction of the model. As **Figure 8(b)** indicates, EGTSyn achieves the best ACC score of 0.71 on the Wang’s dataset and ACC score of 0.53, 0.44 on the Menden’s dataset and Liu’s dataset, respectively. These results infer that the model has certain generalization ability, although there are still some limitations. This may be primarily attributed to the differences in datasets and the lack of diversity of chemical structural SMILES in the training dataset, which can be addressed by using a larger training dataset.

In addition, the EGTSyn model is used for the prediction of synergistic drug combinations, which has not been tested previously. We select 12 drug pairs with high synergy score from (Jaaks et al., 2022) across various cell lines. The results are shown in **Table 7**, where the predicted label and predicted score (i.e., the predicted possibility of drug pairs labeled as 1) are presented. EGTSyn

correctly predict all selected samples, which aligns with the conclusions drawn from (Jaaks et al., 2022). This indicates that the model exhibits good generalization performance and exceptional efficacy in predicting new drug combinations.

4 Discussion

In this study, we introduce a novel EGTSyn model for predicting anti-cancer drug combination synergistic effects. EGTSyn takes advantages of EGNN module and GTD block to extract drug combination features. The EGNN module incorporates the global feature information of the chemicals and the significance of chemical bonds, which is often neglected by previous studies. The GTD block combines EGNN with a Transformer encoder block to extract high-level semantic information of drugs. This design enables EGTSyn to capture the global information of chemicals and the corresponding carcinoma cell line gene profiles, which facilitates a more accurate synergetic judgement of drug combinations. Our ablation study has shown that each design in EGTSyn contributes to the final prediction. Furthermore, we compare EGTSyn to baseline methods, including state-of-the-art models, and show that EGTSyn outperforms these competitive baseline methods. We also verify the superior generalization ability of EGTSyn by testing the model on unseen drug pairs.

Despite the above advantages, the model still has some limitations. Firstly, it does not perform well in generalization testing, which may be attributed to the limited scale of training dataset and the lack of diversity in anti-cancer drugs. Secondly, the high training cost makes it difficult to handle expanding training datasets. Additionally, the neural network architecture and high complexity of the model make it challenging to analyze the interpretability of EGTSyn from a physicochemical mechanism standpoint.

In conclusion, the proposed EGTSyn is of significant and is quite promising for further wet-lab research. In the future, we will design a lightweight model to reduce complexity and incorporate chemical bond information and high-level semantic information to optimize the EGTSyn model. This allows us to train the model on a larger dataset with lower cost and apply it to multi-drug combination synergy prediction tasks as well as other drug combination therapy fields.

5 References

Atz, K., Grisoni, F. and Schneider, G. (2021). Geometric deep learning on molecular representations. *Nature Machine Intelligence*, 3(12), pp.1023-1032. doi: 10.1038/s42256-021-00418-8

Azam, F. and Vazquez, A. (2021). Trends in phase ii trials for cancer therapies. *Cancers*, 13(2), p.178. doi: 10.3390/cancers13020178

Barretina, J., Caponigro, G., Stransky, N., Venkatesan, K., Margolin, A.A., Kim, S., et al. (2012). The Cancer Cell Line Encyclopedia enables predictive modelling of anticancer drug sensitivity. *Nature*, 483(7391), pp.603-607. doi: 10.1038/nature11003

Brandão, M., Pondé, N.F., Poggio, F., Kotecki, N., Salis, M., Lambertini, M., et al. (2018). Combination therapies for the treatment of HER2-positive breast cancer: current and future prospects. *Expert review of anticancer therapy*, 18(7), pp.629-649. doi: 10.1080/14737140.2018.1477596

Bazgir, O., Ghosh, S. and Pal, R. (2021). Investigation of REFINED CNN ensemble learning for anti-cancer drug sensitivity prediction. *Bioinformatics*, 37(Supplement_1), pp. i42-i50. doi: 10.1093/bioinformatics/btab336

Chatterjee, N. and Bivona, T.G. (2019). Polytherapy and targeted cancer drug resistance. *Trends in cancer*, 5(3), pp.170-182. doi: 10.1016/j.trecan.2019.02.003

Cheng, L. and Li, L. (2016). Systematic quality control analysis of LINCS data. *CPT: pharmacometrics & systems pharmacology*, 5(11), pp.588-598. doi: 10.1002/psp4.12107

Ferlay, J., Colombet, M., Soerjomataram, I., Parkin, D.M., Piñeros, M., Znaor, A., et al. (2021). Cancer statistics for the year 2020: An overview. *International journal of cancer*, 149(4), pp.778-789. doi: 10.1002/ijc.33588

Gayvert, K.M., Aly, O., Platt, J., Bosenberg, M.W., Stern, D.F. and Elemento, O. (2017). A computational approach for identifying synergistic drug combinations. *PLoS computational biology*, 13(1), p.e1005308. doi: 10.1371/journal.pcbi.1005803

Hu, J., Gao, J., Fang, X., Liu, Z., Wang, F., Huang, W., et al. (2022). DTsyn: a dual-transformer-based neural network to predict synergistic drug combinations. *Briefings in Bioinformatics*, 23(5), p. bbac302. doi: 10.1093/bib/bbac302

Huang, Y., Jiang, D., Sui, M., Wang, X. and Fan, W. (2017). Fulvestrant reverses doxorubicin resistance in multidrug-resistant breast cell lines independent of estrogen receptor expression. *Oncology reports*, 37(2), pp.705-712. doi: 10.3892/or.2016.5315

Jaaks, P., Coker, E.A., Vis, D.J., Edwards, O., Carpenter, E.F., Leto, S.M., et al. (2022). Effective drug combinations in breast, colon and pancreatic cancer cells. *Nature*, 603(7899), pp.166-173. doi: 10.1038/s41586-022-04437-2

Jiang, P., Huang, S., Fu, Z., Sun, Z., Lakowski, T.M. and Hu, P. (2020). Deep graph embedding for prioritizing synergistic anticancer drug combinations. *Computational and structural biotechnology journal*, 18, pp.427-438. doi: 10.1016/j.csbj.2020.02.006

Kearnes, S., McCloskey, K., Berndl, M., Pande, V. and Riley, P. (2016). Molecular graph convolutions: moving beyond fingerprints. *Journal of computer-aided molecular design*, 30, pp.595-608. doi: 10.1007/s10822-016-9938-8

Kim, Y., Zheng, S., Tang, J., Jim Zheng, W., Li, Z. and Jiang, X. (2021). Anticancer drug synergy prediction in understudied tissues using transfer learning. *Journal of the American Medical Informatics Association*, 28(1), pp.42-51. doi: 10.1093/jamia/ocaa212

Kipf, T.N. and Welling, M. (2016). Semi-supervised classification with graph convolutional networks. *arXiv* [Preprint]. doi: 10.48550/arXiv.1609.02907

Kragh, K.N., Gijón, D., Maruri, A., Antonelli, A., Coppi, M., Kolpen, M., et al. (2021). Effective antimicrobial combination in vivo treatment predicted with microcalorimetry screening. *Journal of Antimicrobial Chemotherapy*, 76(4), pp.1001-1009. doi: 10.1093/jac/dkaa543

Kuru, H.I., Tastan, O. and Cicek, A.E. (2021). MatchMaker: a deep learning framework for drug synergy prediction. *IEEE/ACM Transactions on Computational Biology and Bioinformatics*, 19(4), pp.2334-2344. doi: 10.1109/TCBB.2021.3086702

Landrum, G. (2013). RDKit: A software suite for cheminformatics, computational chemistry, and predictive modeling. *Greg Landrum*, 8.

Liu, Q. and Xie, L. (2021). TranSynergy: mechanism-driven interpretable deep neural network for the synergistic prediction and pathway deconvolution of drug combinations. *PLoS computational biology*, 17(2), p.e1008653. doi: 10.1371/journal.pcbi.1008653

Liu, X., Song, C., Liu, S., Li, M., Zhou, X. and Zhang, W. (2022). Multi-way relation-enhanced hypergraph representation learning for anti-cancer drug synergy prediction. *Bioinformatics*, 38(20), pp.4782-4789. doi: 10.1093/bioinformatics/btac579

Loewe, S. (1953). The problem of synergism and antagonism of combined drugs. *Arzneimittelforschung*, 3, pp.285-290.

Mastropietro, A., Pasculli, G., Feldmann, C., Rodríguez-Pérez, R. and Bajorath, J. (2022). EdgeSHAPer: Bond-centric Shapley value-based explanation method for graph neural networks. *Iscience*, 25(10), p.105043. doi: 10.1016/j.isci.2022.105043

Menden, M.P., Wang, D., Mason, M.J., Szalai, B., Bulusu, K.C., Guan, Y., et al. (2019). Community assessment to advance computational prediction of cancer drug combinations in a pharmacogenomic screen. *Nature communications*, 10(1), p.2674. doi: 10.1038/s41467-019-09799-2

Meng, F., Li, F., Liu, J.X., Shang, J., Liu, X. and Li, Y. (2022). NEXGB: A Network Embedding Framework for Anticancer Drug Combination Prediction. *International Journal of Molecular Sciences*, 23(17), p.9838. doi: 10.3390/ijms23179838

Nakano, T. and JB, B. (2020). Prediction of Compound Cytotoxicity Based on Compound Structures and Cell Line Molecular Characteristics. *Journal of Computer Aided Chemistry*, 21, pp.1-10. doi: 10.2751/jcac.21.1

Nguyen, T., Le, H., Quinn, T.P., Nguyen, T., Le, T.D. and Venkatesh, S. (2021). GraphDTA: predicting drug-target binding affinity with graph neural networks. *Bioinformatics*, 37(8), pp.1140-1147. doi: 10.1093/bioinformatics/btaa921

O'Neil, J., Benita, Y., Feldman, I., Chenard, M., Roberts, B., Liu, Y., et al. (2016). An unbiased oncology compound screen to identify novel combination strategies. *Molecular cancer therapeutics*, 15(6), pp.1155-1162. doi: 10.1158/1535-7163.MCT-15-0843

Preto, A.J., Matos-Filipe, P., Mourão, J. and Moreira, I.S. (2022). SYNPRED: prediction of drug combination effects in cancer using different synergy metrics and ensemble learning. *GigaScience*, 11. doi: 10.1093/gigascience/giac087

Preuer, K., Lewis, R.P., Hochreiter, S., Bender, A., Bulusu, K.C. and Klambauer, G. (2018). DeepSynergy: predicting anti-cancer drug synergy with Deep Learning. *Bioinformatics*, 34(9), pp.1538-1546. doi: 10.1093/bioinformatics/btx806

Ribas, A., Lawrence, D., Atkinson, V., Agarwal, S., Miller Jr, W.H., Carlino, M.S., et al. (2019). Combined BRAF and MEK inhibition with PD-1 blockade immunotherapy in BRAF-mutant melanoma. *Nature medicine*, 25(6), pp.936-940. doi: 10.1038/s41591-019-0476-5

Roell, K.R., Reif, D.M. and Motsinger-Reif, A.A. (2017). An introduction to terminology and methodology of chemical synergy—perspectives from across disciplines. *Frontiers in pharmacology*, 8, p.158. doi: 10.3389/fphar.2017.00158

Rong, Y., Bian, Y., Xu, T., Xie, W., Wei, Y., Huang, W., et al. (2020). Self-supervised graph transformer on large-scale molecular data. *Advances in Neural Information Processing Systems*, 33, pp.12559-12571.

Torres, N.P., Lee, A.Y., Giaever, G., Nislow, C. and Brown, G.W. (2013). A high-throughput yeast assay identifies synergistic drug combinations. *Assay and drug development technologies*, 11(5), pp.299-307.

Vaswani, A., Shazeer, N., Parmar, N., Uszkoreit, J., Jones, L., Gomez, A.N., et al. (2017). Attention is all you need. *Advances in neural information processing systems*, 30.

Wang, J., Liu, X., Shen, S., Deng, L. and Liu, H. (2022). DeepDDS: deep graph neural network with attention mechanism to predict synergistic drug combinations. *Briefings in Bioinformatics*, 23(1), p.bbab390. doi: 10.1093/bib/bbab390

Wang, Z., Chen, J. and Chen, H. (2021). EGAT: Edge-featured graph attention network. In Artificial Neural Networks and Machine Learning–ICANN 2021: 30th International Conference on Artificial Neural Networks, Bratislava, Slovakia, September 14–17, 2021, Proceedings, Part I 30 (pp. 253-264). doi: 10.1007/978-3-030-86362-3_21

Weininger, D. (1988). SMILES, a chemical language and information system. 1. Introduction to methodology and encoding rules. *Journal of chemical information and computer sciences*, 28(1), pp.31-36. doi: 10.1021/ci00057a005

Westerweel, P.E., Te Boekhorst, P.A., Levin, M.D. and Cornelissen, J.J. (2019). New approaches and treatment combinations for the management of chronic myeloid leukemia. *Frontiers in oncology*, 9, p.665. doi: 10.3389/fonc.2019.00665

Wishart, D.S., Feunang, Y.D., Guo, A.C., Lo, E.J., Marcu, A., Grant, J.R., et al. (2018). DrugBank 5.0: a major update to the DrugBank database for 2018. *Nucleic acids research*, 46(D1), pp. D1074-D1082. doi: 10.1093/nar/gkx1037

Xiong, R., Yang, Y., He, D., Zheng, K., Zheng, S., Xing, C., et al. (2020), November. On layer normalization in the transformer architecture. In *International Conference on Machine Learning* (pp. 10524-10533). PMLR.

Xu, J. and Qiu, Y. (2019). Current opinion and mechanistic interpretation of combination therapy for castration-resistant prostate cancer. *Asian Journal of Andrology*, 21(3), p.270. doi: 10.4103/aja.aja_10_19

Yang, J., Xu, Z., Wu, W.K.K., Chu, Q. and Zhang, Q. (2021). GraphSynergy: a network-inspired deep learning model for anticancer drug combination prediction. *Journal of the American Medical Informatics Association*, 28(11), pp.2336-2345. doi: 10.1093/jamia/ocab162

Yang, Y. and Li, D. (2020). Nenn: Incorporate node and edge features in graph neural networks. In *Asian conference on machine learning* (pp. 593-608). PMLR.

Yang, W., Soares, J., Grenninger, P., Edelman, E.J., Lightfoot, H., Forbes, S., et al. (2012). Genomics of Drug Sensitivity in Cancer (GDSC): a resource for therapeutic biomarker discovery in cancer cells. *Nucleic acids research*, 41(D1), pp. D955-D961. doi: 10.1093/nar/gks1111

Ying, C., Cai, T., Luo, S., Zheng, S., Ke, G., He, D., et al. (2021). Do transformers really perform badly for graph representation? *Advances in Neural Information Processing Systems*, 34, pp.28877-28888.

Yu, S., Kim, T., Yoo, K.H. and Kang, K. (2017). The T47D cell line is an ideal experimental model to elucidate the progesterone-specific effects of a luminal A subtype of breast cancer. *Biochemical and Biophysical Research Communications*, 486(3), pp.752-758. doi: 10.1016/j.bbrc.2017.03.114

Zagidullin, B., Aldahdooh, J., Zheng, S., Wang, W., Wang, Y., Saad, J., et al. (2019). DrugComb: an integrative cancer drug combination data portal. *Nucleic acids research*, 47(W1), pp. W43-W51. doi: 10.1093/nar/gkz337

Zagidullin, B., Wang, Z., Guan, Y., Pitkänen, E. and Tang, J. (2021). Comparative analysis of molecular fingerprints in prediction of drug combination effects. *Briefings in bioinformatics*, 22(6), p. bbab291. doi: 10.1093/bib/bbab291

6 Figures

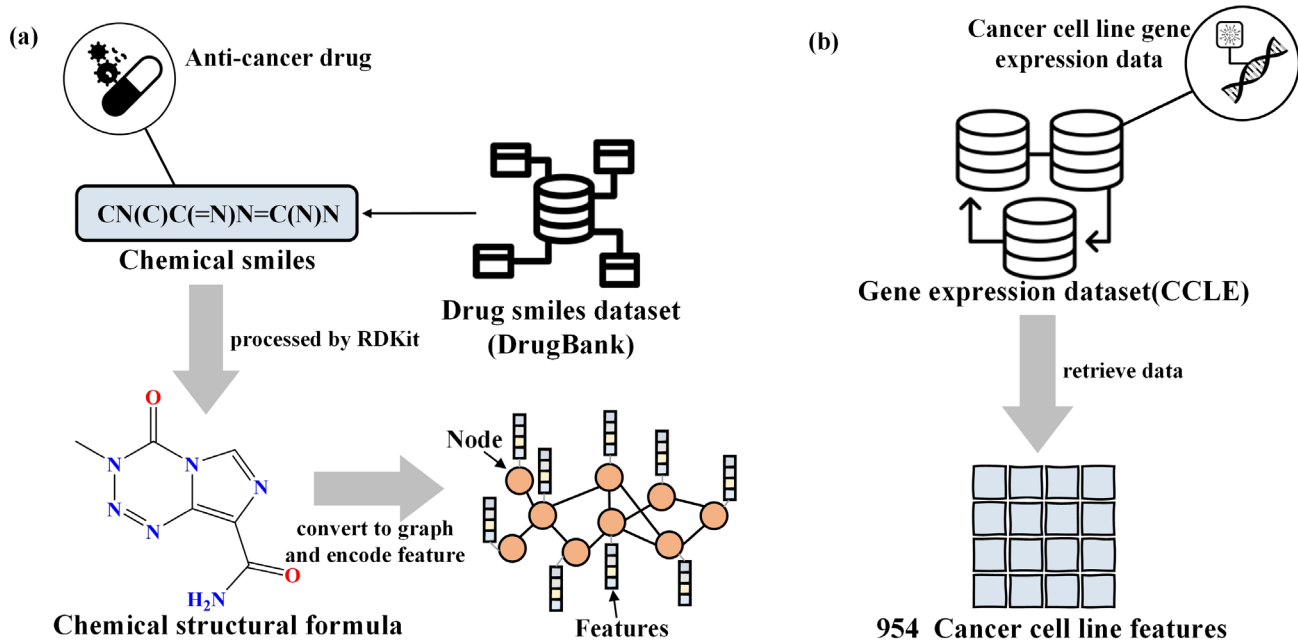


Figure 1. Data collections description. (a) Drug features formulation. (b) Cancer cell line feature retrieval.

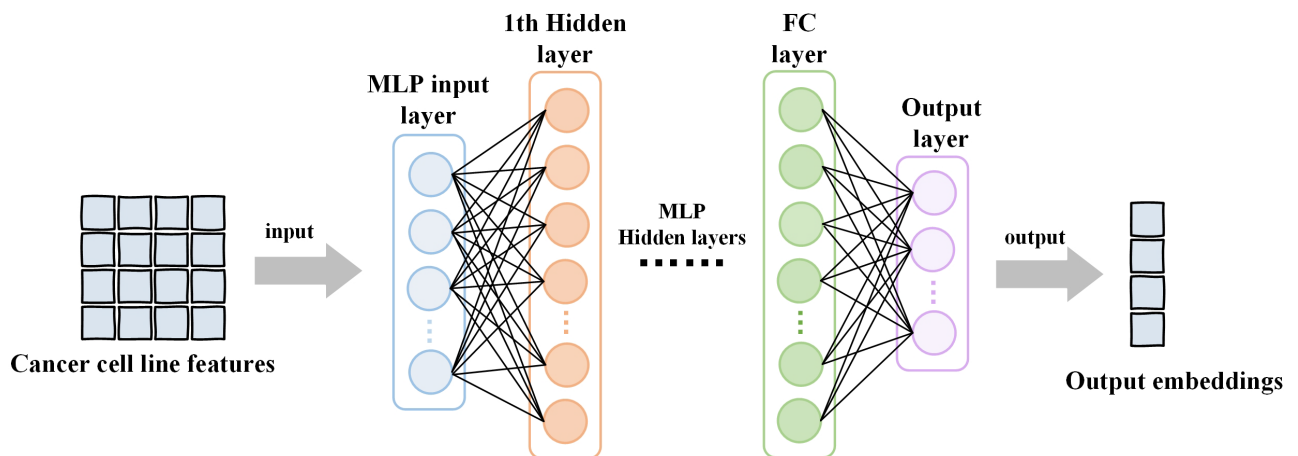


Figure 2. Illustration of cell feature reduction block.

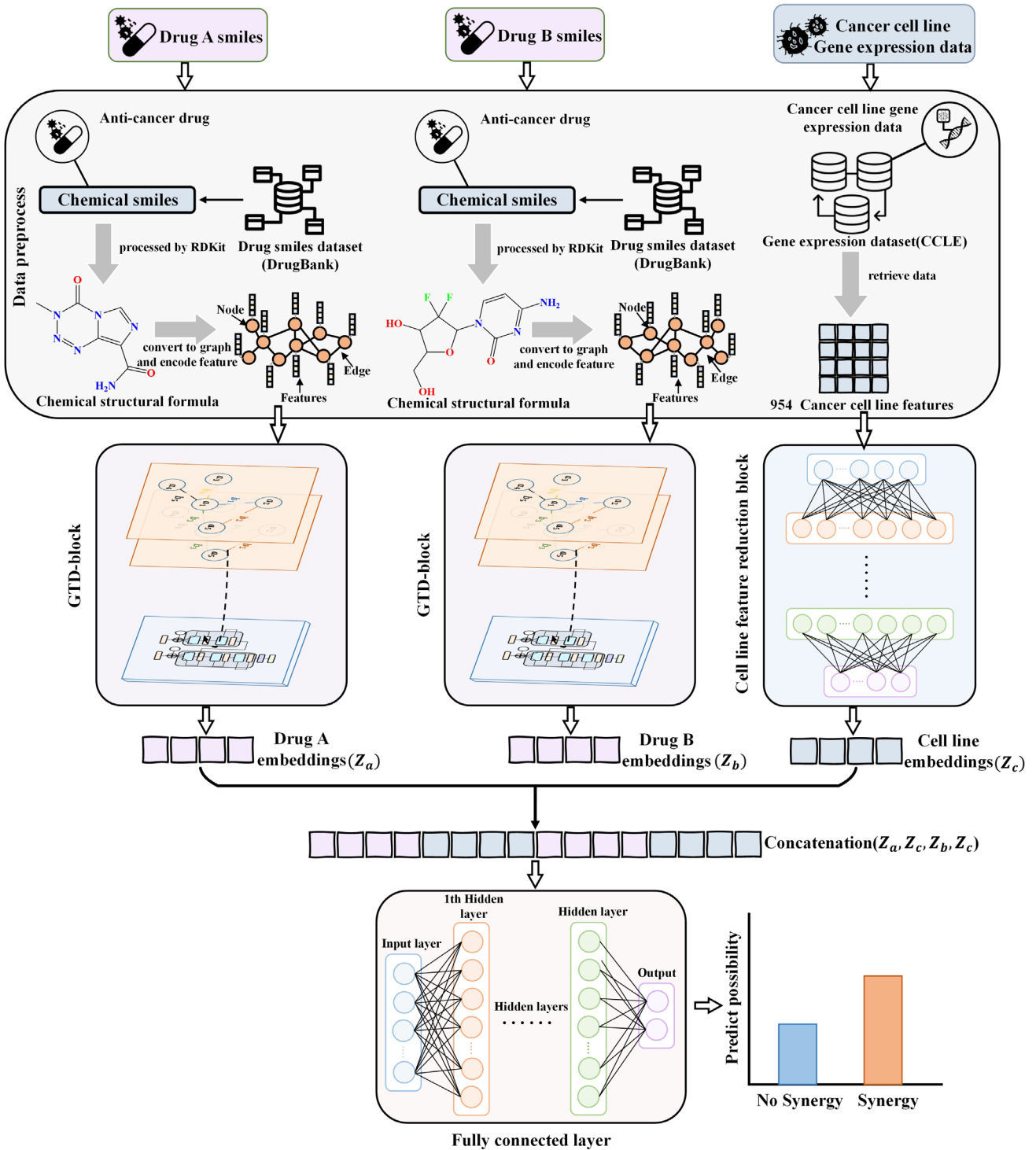


Figure 3. The framework of EGTSyn. The chemical structural SMILES of each drug are pipelined by a GTDblock and then be concatenated with cancer cell line features that calculated by a feature reduction block, respectively. The above two drug-cell feature representation vectors will be further concatenated to serve as input for the final classify layers.

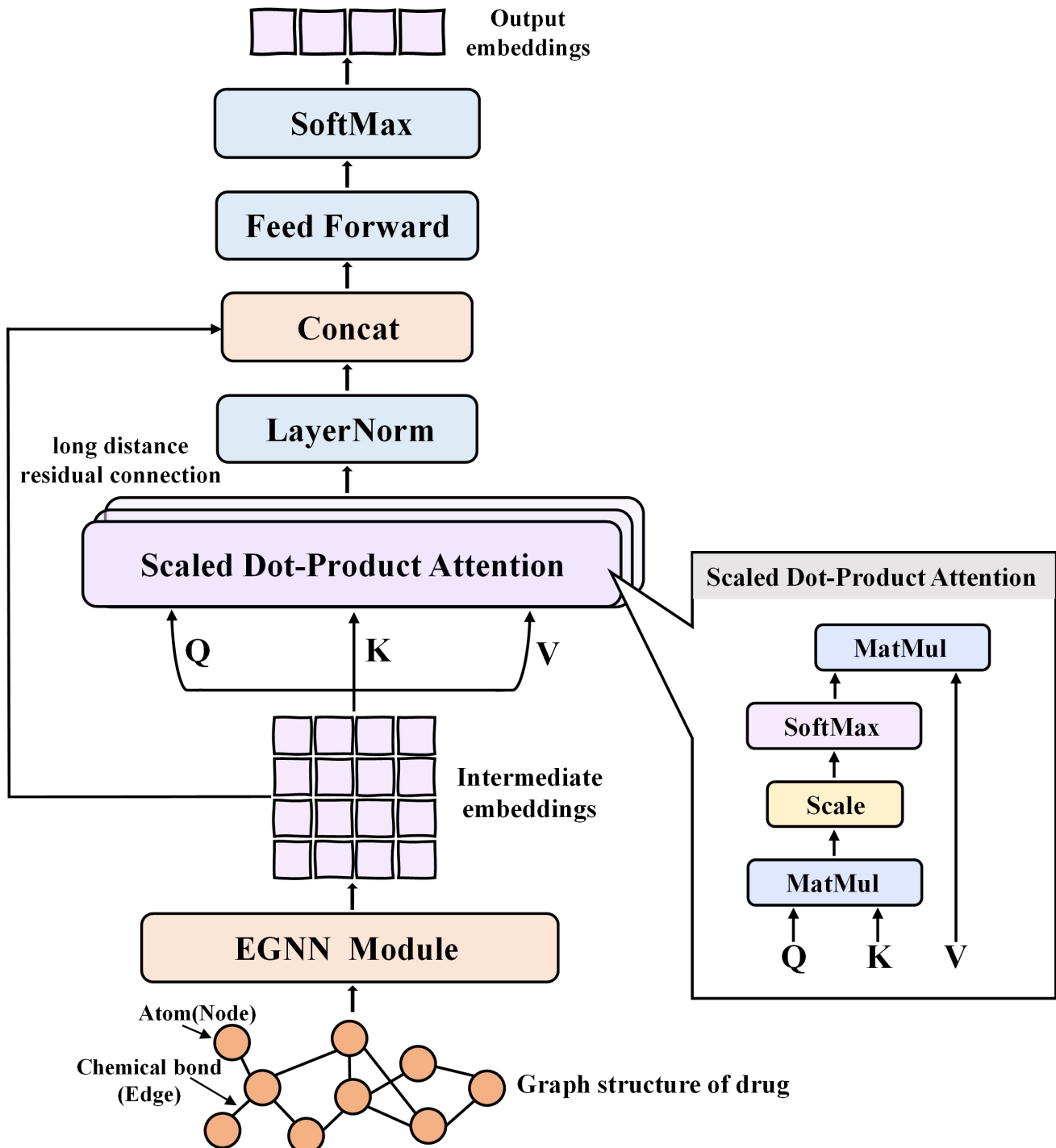


Figure 4. The framework of GTDblock. The converted graphs serve as the input of GTDblock and then be calculated by EGNN module. The intermediate output embeddings will be further duplicated triply as K, Q and V for the following transformer encoder block. Additionally, a long-distance residual connection is also applied to convey low-level structure information.

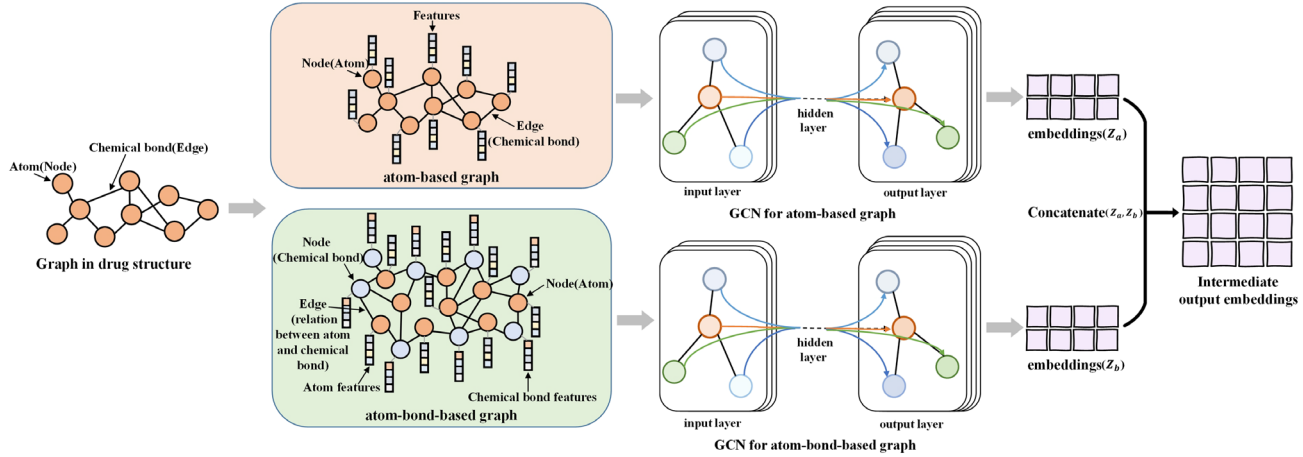


Figure 5. The structure of EGNN. EGNN takes atom-based graph and atom-bond-based graph as inputs. The two graphs are processed by two identical structured GCNs, respectively. The two output embeddings are concatenated together to formulate the intermediate embeddings for the following transformer encoder block.

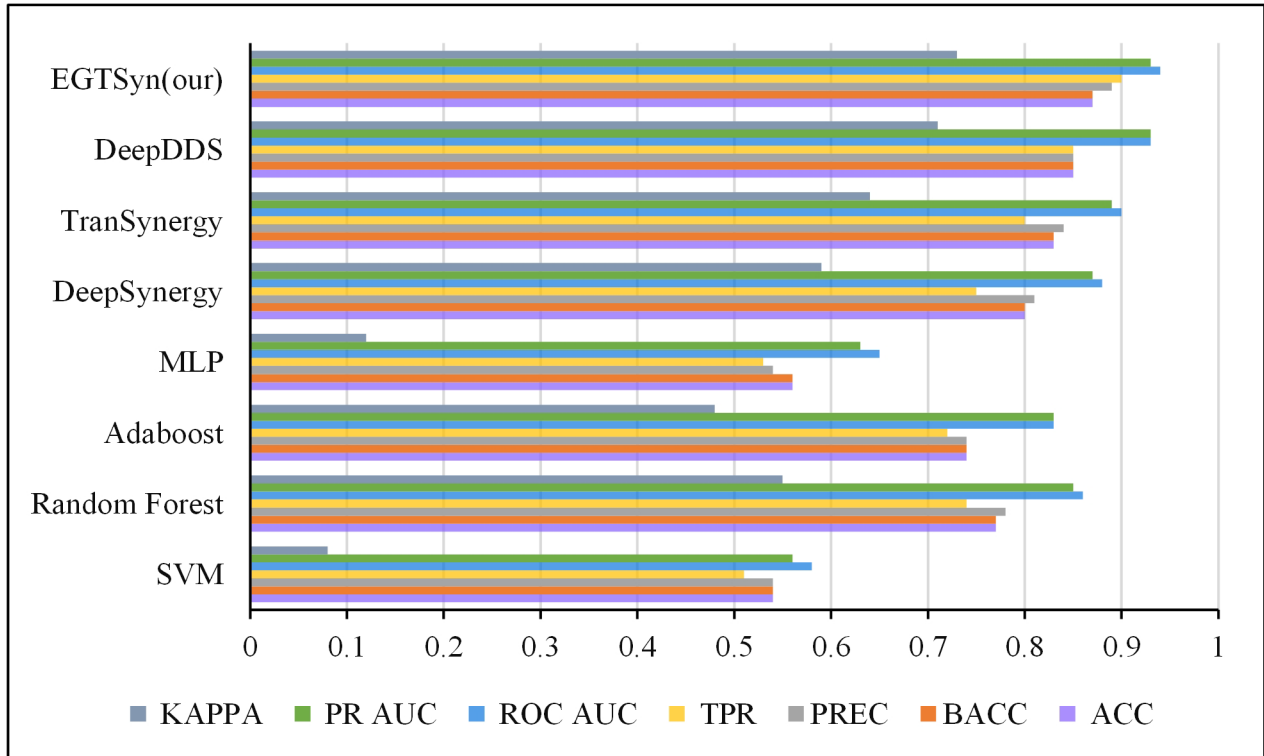


Figure 6. Performance Comparison of EGTSyn with baseline methods upon the random split 5-folds cross validation.

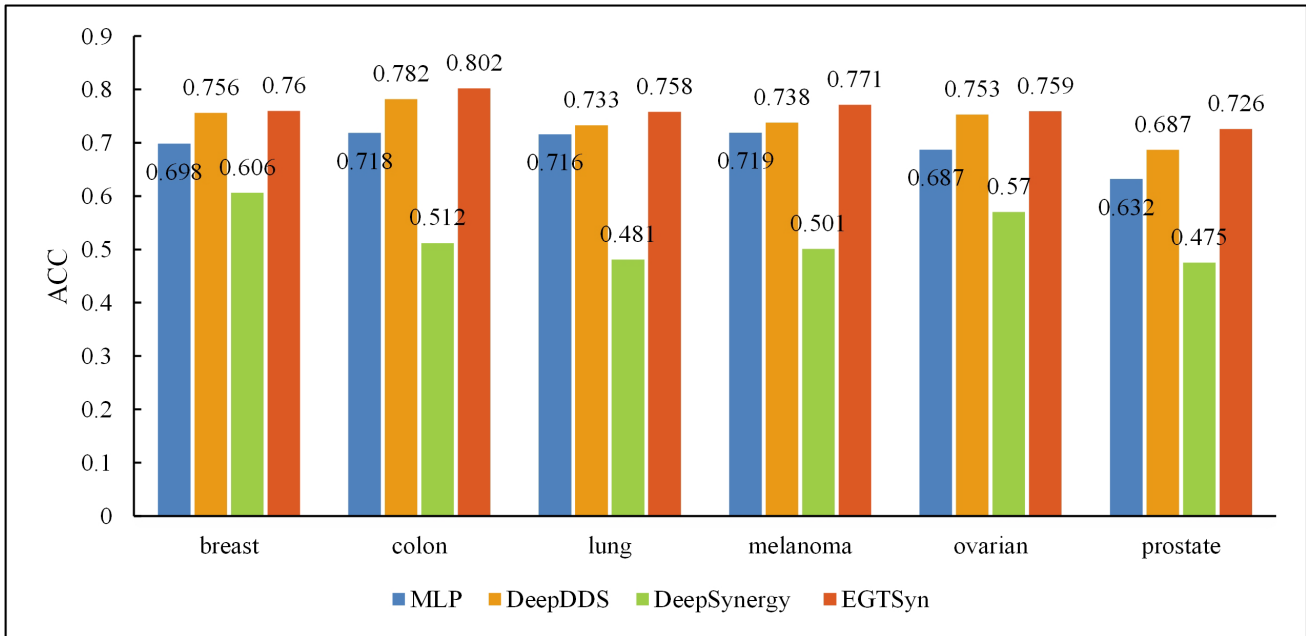


Figure 7. ACC metric of MLP, DeepDDS, DeepSynergy and EGTSyn on six different tissues: breast, colon, lung, melanoma, ovarian, prostate.

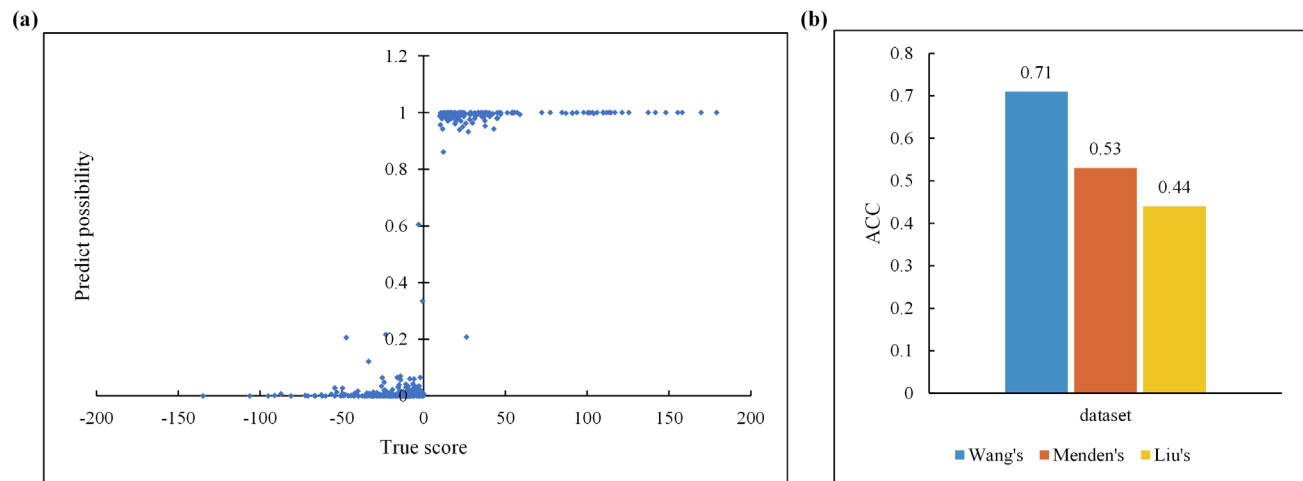


Figure 8. (a) Scatter plot of predict possibility of synergy scores. The horizontal axis denotes true synergy score, and vertical axis denotes the possibility of drug pairs being predicted as synergistic by our model. (b) Generalization performance validation of EGTSyn on three new datasets. The horizontal axis denotes three datasets and the vertical axis denotes the ACC (accuracy) scores on each dataset.

7 Tables

Table 1. Details for atom features.

Feature Representation	Explanation
Atom symbol	C,N,O,S,F,Si,P,Cl,Br,Mg,Na,Ca,Fe,In,Mn,As,Al,I,B,V,K,Tl,Yb,Sb,Sn,Ag,Pd,Zr,Cr,Co,Se,Ti,Zn,H,Li,Ge,Cu,Au,Ni,Cd,Pt,Hg,Pb,Unknown
Adjacent atoms	Number of atom neighbors that directly connected
Aromaticity	Whether this atom is part of an aromatic system
Valence	Explicit valence of the atom
Adjacent hydrogen	Number of directly connected Hydrogen atom

Table 2. Details for bond features.

Feature Representation	Explanation
Bond type	Single, double, triple, or others
Direction	direction of bond: upright, downright, or none
Conjugation	Whether the bond is part of a conjugated system
Aromaticity	Whether the bond is part of an aromatic system
Ring	Whether the bond is part of a specific ring
Owning mol	Whether the bond is part of a specific molecule

Table 3. Hyperparameter settings of EGTSyn.

Hyperparameter	Values
EGCN layer	1; 2; 3
Size of EGCN	78 ; 128; 256
Hidden size of GTDblock	156 ; 256; 512
Number of attention heads	1; 2; 4; 8 ; 16; 32
MLP hidden size	[1024,512]; [2048,512]; [2048,1024];
Hidden units of final linear block	[1024,512,128] ; [2048, 1024, 512]; [4096, 1024, 512]
Dropout rate	0.1; 0.2 ; 0.3; 0.4; 0.5
Learning rate	1e-1; 1e-3; 5e-3; 4e-4 ; 1e-5; 5e-5
Graph pooling method	sum; mean; max

Table 4. Performance Comparison of EGTSyn with baseline methods upon the random split 5-folds cross validation.

Metrics	ACC	BACC	PREC	TPR	ROC AUC	PR AUC	KAPPA
SVM	0.54±0.01	0.54±0.01	0.54±0.01	0.51±0.12	0.58±0.01	0.56±0.02	0.08±0.04
Random Forest	0.77±0.01	0.77±0.01	0.78±0.02	0.74±0.01	0.86±0.02	0.85±0.02	0.55±0.04
Adaboost	0.74±0.01	0.74±0.02	0.74±0.02	0.72±0.01	0.83±0.01	0.83±0.03	0.48±0.03
MLP	0.56±0.06	0.56±0.05	0.54±0.04	0.53±0.22	0.65±0.02	0.63±0.05	0.12±0.04
DeepSynergy	0.80±0.01	0.80±0.01	0.81±0.01	0.75±0.01	0.88±0.01	0.87±0.01	0.59±0.05
TranSynergy	0.83±0.01	0.83±0.01	0.84±0.01	0.80±0.01	0.90±0.01	0.89±0.01	0.64±0.01
DeepDDS	0.85±0.07	0.85±0.07	0.85±0.07	0.85±0.07	0.93±0.01	0.93±0.01	0.71±0.21
EGTSyn (Our)	0.87±0.08	0.87±0.08	0.89±0.08	0.90±0.09	0.94±0.05	0.93±0.03	0.73±0.01

Table 5. Performance Comparison of EGTSyn with baseline methods upon leave-drug-out, leave-tissue-out, leave-drug combination-out validation.

Experiment	Leave-drug-out			Leave-tissue-out			Leave-drug combination-out		
Metrics	ROC AUC	PR AUC	ACC	ROC AUC	PR AUC	ACC	ROC AUC	PR AUC	ACC
SVM	0.60±0.02	0.59±0.05	0.55±0.03	0.66±0.04	0.66±0.07	0.59±0.05	0.66±0.01	0.65±0.05	0.58±0.01
Random Forest	0.67±0.08	0.66±0.05	0.62±0.06	0.80±0.08	0.80±0.05	0.71±0.05	0.82±0.02	0.81±0.03	0.74±0.02
Adaboost	0.62±0.11	0.61±0.06	0.58±0.11	0.77±0.12	0.78±0.11	0.70±0.11	0.77±0.02	0.78±0.02	0.69±0.03
MLP	0.69±0.05	0.68±0.04	0.62±0.06	0.77±0.07	0.76±0.05	0.70±0.06	0.82±0.03	0.81±0.05	0.74±0.02
DeepSynergy	0.71±0.07	0.64±0.06	0.61±0.07	0.80±0.01	0.79±0.04	0.71±0.05	0.83±0.03	0.81±0.05	0.77±0.03
TranSynergy				0.81±0.01	0.79±0.02	0.73±0.03			
DeepDDS	0.73±0.01	0.72±0.05	0.66±0.02	0.83±0.04	0.82±0.4	0.74±0.03	0.89±0.02	0.88±0.06	0.81±0.03
EGTSyn (Our)	0.75±0.02	0.73±0.02	0.68±0.02	0.84±0.02	0.84±0.03	0.76±0.02	0.88±0.01	0.88±0.02	0.81±0.01

Table 6. Results of ablation studies.

	ROC AUC	PR AUC	ACC	BACC	KAPPA
EGTSyn	0.94±0.05	0.93±0.03	0.87±0.08	0.87±0.08	0.73±0.01
GTSyn	0.93±0.04	0.93±0.07	0.86±0.07	0.86±0.07	0.72±0.01
EGSyn	0.93±0.02	0.93±0.04	0.85±0.04	0.86±0.04	0.71±0.08
GSyn	0.92±0.04	0.92±0.05	0.85±0.06	0.85±0.06	0.70±0.01

Table 7. Predicted results on 12 synergistic drug combinations.

drug A	drug B	cell line	predict score	predict label	true label
Navitoclax	Paclitaxel	PANC0403	0.9922	1	1
SCH772984	Taselisib	SUIT2	0.9733	1	1
AZD7762	Camptothecin	HDQP1	0.9757	1	1
Navitoclax	Tozasertib	MCF7	0.9961	1	1
Navitoclax	Alisertib	HCC1599	0.9556	1	1
Navitoclax	GSK269962A	BT474	0.6969	1	1
Navitoclax	ZM447439	AU565	0.9615	1	1
Taselisib	Trametinib	HT115	0.9956	1	1
Linsitinib	Sapitinib	SKCO1	0.7493	1	1
AZD4547	Sapitinib	LS123	0.6616	1	1
AZD7762	Gemcitabine	PANC0327	0.501	1	1
Crizotinib	Lapatinib	MZ1PC	0.9717	1	1